Clinical Cancer Research

Bortezomib Treatment Sensitizes Oncolytic HSV-1–Treated Tumors to NK Cell Immunotherapy

Ji Young Yoo[1], Alena Cristina Jaime-Ramirez[1], Chelsea Bolyard[1], Hongsheng Dai[2], Tejaswini Nallanagulagari[1,3,4], Jeffrey Wojton[1,5], Brian S. Hurwitz[1,6], Theresa Relation[1,7], Tae Jin Lee[8], Michael T. Lotze[9], Jun-Ge Yu[10], Jianying Zhang[11], Carlo M. Croce[8], Jianhua Yu[2], Michael A. Caligiuri[2], Matthew Old[10], and Balveen Kaur[1]

Abstract

Purpose: Both the proteasome inhibitor bortezomib and an oncolytic herpes simplex virus-1 (oHSV)–expressing GM-CSF are currently FDA approved. Although proteasome blockade can increase oHSV replication, immunologic consequences, and consequent immunotherapy potential are unknown. In this study, we investigated the impact of bortezomib combined with oHSV on tumor cell death and sensitivity to natural killer (NK) cell immunotherapy.

Experimental Design: Western blot, flow cytometry, and caspase 3/7 activity assays were used to evaluate the induction of apoptosis/autophagy and/or necroptotic cell death. Cellular and mitochondrial reactive oxygen species (ROS) production was measured using CellROX and MitoSOX. Inhibitors/shRNA–targeting ROS, JNK and RIP1 kinase (RIPK1) were used to investigate the mechanism of cell killing. The synergistic interaction between oHSV and bortezomib was calculated using a Chou–Talalay analysis. NK cells isolated from normal human blood were co-cultured with tumor cells to evaluate cellular interactions. Q-PCR, ELISA, and FACS analysis were used to evaluate NK cell activation. Intracranial tumor xenografts were used to evaluate antitumor efficacy.

Results: Combination treatment with bortezomib- and oHSV-induced necroptotic cell death and increased the production of mitochondrial ROS and JNK phosphorylation. Inhibitors/shRNA of RIPK1 and JNK rescued synergistic cell killing. Combination treatment also significantly enhanced NK cell activation and adjuvant NK cell therapy of mice treated with bortezomib and oHSV improved antitumor efficacy.

Conclusions: This study provides a significant rationale for triple combination therapy with bortezomib, oHSV, and NK cells to improve efficacy, in glioblastoma patients. *Clin Cancer Res; 22(21); 5265–76. ©2016 AACR.*

See related commentary by Suryadevara et al., p. 5164

Introduction

Oncolytic herpes simplex virus-1 (oHSV) specifically targets and kills tumors cells and is currently being evaluated for safety and efficacy in multiple clinical trials (1). The recent FDA approval of T-Vec, an oHSV for advanced non-resectable melanoma, underscores the potential of this biological treatment for therapy-resistant cancers (2, 3). A better understanding of the oHSV interactions with approved chemotherapy agents can help design more efficacious therapeutic strategies to combat cancer.

Increased protein synthesis and degradation are required for aggressive tumor growth, and are hallmarks of cancer (4). There are two major cellular pathways of protein degradation in eukaryotic cells: the ubiquitin-proteasome system (UPS) and the autophagy-lysosome system (autophagy). UPS-mediated proteolysis involves initial ubiquitination followed by proteasome-mediated degradation of targeted proteins. Thus, specific chemical inhibitors of the proteasome have emerged as effective anti-tumor drugs (2).

Bortezomib is a peptide-based, reversible inhibitor of the 26-S proteasome and is currently FDA approved for use in multiple myeloma and mantle cell lymphoma. We have previously demonstrated that induction of the unfolded protein response (UPR) in tumor cells (glioma, head and neck, and ovarian) after bortezomib treatment led to an increase of heat shock protein 90 (HSP90), which supported increased viral replication via

[1]Department of Neurological Surgery, Dardinger Laboratory for Neuro-oncology and Neurosciences, The Ohio State University Wexner Medical Center, Columbus, Ohio. [2]Division of Hematology, Department of Internal Medicine, The Ohio State University Wexner Medical Center, Columbus, Ohio. [3]Department of Chemistry and Biochemistry, The Ohio State University Wexner Medical Center, Columbus, Ohio. [4]Department of Microbiology, The Ohio State University Wexner Medical Center, Columbus, Ohio. [5]Neuroscience Graduate Studies Program, The Ohio State University Wexner Medical Center, Columbus, Ohio. [6]Department of Biomedical Science Major, The Ohio State University Wexner Medical Center, Columbus, Ohio. [7]Medical Scientist Training Program, The Ohio State University Wexner Medical Center, Columbus, Ohio. [8]Department of Cancer Biology and Genetics, The Ohio State University Wexner Medical Center, Columbus, Ohio. [9]Departments of Surgery, Immunology, and Bioengineering, University of Pittsburgh School of Medicine, Pittsburgh, Pennsylvania University of Pittsburgh Cancer Institute, Pittsburgh, Pennsylvania. [10]Department of Otolaryngology, Head and Neck Surgery, The Ohio State University Wexner Medical Center, Columbus, Ohio. [11]Department of Biomedical Informatics, Center for Biostatistics, James Comprehensive Cancer Center, The Ohio State University Wexner Medical Center, Columbus, Ohio.

Note: Supplementary data for this article are available at Clinical Cancer Research Online (http://clincancerres.aacrjournals.org/).

Corresponding Authors: Balveen Kaur, The Ohio State University, 400 West 12th Avenue, 385 B Wiseman Hall, Columbus, OH 43210. Phone: 614-292-3984; Fax: 614-688-4882; E-mail: balveen.kaur@osumc.edu; and Ji Young Yoo, The Ohio State University, 400 West 12th Avenue, 352 Wiseman Hall, Columbus, OH 43210. Phone: 614-292-1321; Fax: 614-688-4882; E-mail: Jiyoung.Yoo@osumc.edu

doi: 10.1158/1078-0432.CCR-16-1003

Translational Relevance

Oncolytic virus (OV) therapy has emerged as a promising biological therapy with many potential applications. FDA approval of first oncolytic HSV (oHSV; Imlygic), for use in advanced melanoma, highlights its relevance in cancer. Using a combination treatment modality with bortezomib, an FDA-approved peptide-based reversible proteasome inhibitor, we found that oHSV induced inflammatory necroptotic cell death accompanied by the secretion of inflammatory cytokines into the tumor microenvironment. This resulted in natural killer (NK) cell activation and increased sensitization of infected tumor cells to NK cell–mediated killing. Furthermore, using primary human NK cells and *in vivo* models, bortezomib and oHSV combination treatment sensitized tumor cells to primary NK cell immunotherapy, resulting in increased tumor killing and murine survival. Because proteasome inhibitors, oHSVs, and autologous NK cell immunotherapy are currently being investigated individually in GBM patients, our study provides the rationale for combining these therapies in future clinical trials.

enhanced nuclear location of the viral polymerase *in vitro*. This resulted in synergistic cancer cell killing *in vitro*, and treatment of mice with bortezomib and oHSV resulted in improved antitumor efficacy *in vivo* (3). Because proteasome blockade results in apoptotic cell death and oHSV has evolved several mechanisms to block apoptosis, here, we evaluated the consequences of infecting bortezomib-treated cells with an oHSV and its effect on cellular death.

We observed that treatment of tumor cells with bortezomib before oHSV infection resulted in a RIPK1-dependent necroptotic cell death, leading to JNK-dependent reactive oxygen species (ROS) production. This increased necroptotic cell death was accompanied by enhanced proinflammatory cytokine induction and secretion, which could be harnessed to activate an antitumor immune response. Furthermore, combination therapy led to increased cell surface expression of NK cell activating markers on tumor cells. Co-culture of primary human NK cells with combination treated tumor cells increased NK cell TRAIL expression, which together enhanced NK cell activation and NK cell–mediated tumor cell killing. *In vivo* antitumor efficacy corroborated that proteasome blockade in conjunction with oncolysis set up the stage for efficient NK cell–mediated tumor cell killing, resulting in improved overall survival of tumor-bearing mice. These findings support the translation of this triple treatment strategy in glioblastoma patients.

Materials and Methods

Cell lines and HSV

U251T3, LN229, T98G, X12V2, U87ΔEGFR, and Vero were maintained in DMEM (Gibco BRL) supplemented with 10% FBS. U251 cells were obtained from Dr. Erwin G. Van Meir (Emory University) and U251T3 cells were created in our laboratory (May 2009) as a tumorigenic clone of U251 cells by serially passaging these cells three times in mice. LN229 and T98G cells were obtained in January 2005 from Erwin G. Van Meir (Emory University). U87ΔEGFR cell line expresses a truncated, constitutively active, mutant form of epidermal growth factor receptor (EGFRvIII), and has been previously described (5). Monkey kidney epithelial derived Vero cells have not been authenticated since receipt. U87ΔEGFR (January 2015), LN229 (July 2013), U251T3 (January 2015), T98G (January 2015), X12V2 (August, 2015) cells were authenticated by the University of Arizona Genetics Core via STR profiling. All cell lines were maintained at 37°C in a humidified atmosphere with 5% carbon dioxide and maintained with 100 U of penicillin/mL, and 0.1 mg of streptomycin/mL (Pen/Strep). Cells are routinely monitored for changes in morphology and growth rate. All cells were negative for *Mycoplasma*. The construction and generation of 34.5ENVE has been previously described and virus was prepared and titered as previously described (6, 7). Virus was propagated in Vero cells as described previously (8).

Cell killing assay

The cytotoxicity of bortezomib and 34.5ENVE was determined in each cell line by measuring the conversion of the tetrazolium salt MTT to formazan (MTT assay) as described (3). On the basis of the calculated ED_{50} of each agent, bortezomib and 34.5ENVE were diluted 0.0625, 0.125, 0.25, 0.5, 1, 2, and 4 times in a constant ratio. Cells were plated onto 96-well plates at approximately 50% confluence and pretreated with serially diluted concentrations of bortezomib for 16 hours, then washed before the addition of serially diluted oHSV. Seven-two hours after infection, cells were treated with 10 μL of the MTT-labeling reagent and were gently shaken and incubated at 37°C in a 5% CO_2 incubator. Four hours later, 100 μL of solubilization solution was added and incubated overnight to solubilize. Plates were read on the next day using a microplate reader at 590 nm. All assays were performed in triplicate. Combination indices were calculated using compusyn program. For rescue assays with necrostatin-1 (nec-1) or JNK inhibitor (SP0600125), cells were pretreated with nec-1 or SP0600125 before bortezomib treatment.

Flow cytometric analysis

Apoptosis and necrosis were quantified by double staining with Annexin-V and 7AAD then analyzed by flow cytometry using a Becton Dickinson FACS LSRII flow cytometer (Becton-Dickinson) as previously described (9). U251T3 cells were pretreated with 12 nmol/L bortezomib for 16 hours. Two-four hours later, cells were washed and infected with PBS or 34.5ENVE at an MOI of 0.01. Twenty-four hours after virus infection, cells were processed according to the manufacturer's instruction in the PE Annexin V Apoptosis Detection Kit (BD Biosciences Pharmingen). Apoptosis was quantified on a FACS LSRII (Becton Dickinson), and data from 10,000 events were collected for further analysis.

Caspase 3/7 assay

Caspase-3 and -7 activities were measured at 24 hours using the Caspase 3/7 Kit (Caspase-Glo 3/7 Assay, cat. no. G8091, Promega). This assay kit provides a proilluminescent Caspase 3/7 substrate, which contains the tetrapeptide sequence DEVD that is cleaved to release aminoluciferin. U251T3 cells were plated at 1×10^4 cells per well in 96-well plates and treated with 12 nmol/L of bortezomib. Twenty-four hours later, 0.01 MOI of oHSV was added to the cells. Twenty-four hours after oHSV infection, 100 μL of Caspase 3/7 substrate was added to the cells for one hour and

luminescence was measured by a Fluostar Optima plate reader (BMG Labtech) in triplicate as directed by the manufacturer (7).

Western blot analysis and antibodies

Cell lysates were fractionated by SDS-PAGE and transferred to polyvinylidene difluoride (PVDF) membranes. Blocked membranes were then incubated with antibodies against anti-cleaved caspase-3, caspase-8, LC3B, Rip1, phospho-JNK, and total JNK (Cell Signaling Technology), phosphorylated c-Jun (pS63), and total c-Jun (BD Biosciences Pharmingen), GAPDH (Abcam; each diluted 1:1,000), horseradish peroxidase (HRP)–conjugated secondary anti-mouse antibody (each diluted 1:1,000; GE Healthcare), HRP-conjugated secondary goat anti-rabbit antibody (each diluted 1:1,000; Dako), and the immunoreactive bands were visualized using enhanced chemiluminescence (ECL; GE Healthcare).

Intracellular and mitochondria-specific ROS measurement

Intracellular- and mitochondria-specific ROS were measured using the cell-permeable CellROX Deep Red (Invitrogen) and MitoSOX Red Reagent (Invitrogen) that are fluorogenic probes designed to measure ROS in living cells. Cells were pretreated with 12 nmol/L bortezomib for 16 hrs. The next day, cells were washed and infected with PBS or 34.5ENVE at an MOI of 0.01. Twenty-four hours after viral infection, 5 μL of CellROX Deep Red or MitoSOX Red Reagent was added to each sample and incubated at 37°C for 30 minutes. ROS was quantified on a Becton Dickinson FACS Calibur flow cytometer (Becton Dickinson) as previously described (10).

Quantification of human IL1α, IFNγ, and TNFα by ELISA

Human IL1α, IFNγ, and TNFα (DuoSet ELISA kit; R&D Systems) were quantified in cell supernatants with/without co-cultured with primary NK cells or treated mice serum according to the manufacturer's recommendations.

Isolation of NK cells from human donors

NK cells were isolated from fresh peripheral blood leukopacks (American Red Cross) by 30-minute incubation with RossetteSep cocktail (Stem Cell Technologies) before Ficoll Hypaque (Sigma) density gradient centrifugation. NK cells were then cultured in 10% FBS RPMI media and used in downstream applications.

Live/dead cell staining cytotoxicity assay with NK Cells

U251T3-mCherry cells, which stably express mCherry, were plated overnight at 3×10^5 cells per well. Where noted, cells were treated with/without ED_{50} bortezomib for 16 hours before infection, washed, and then infected with 34.5ENVE. Cells were infected for 2 hours with 34.5ENVE (MOI = 0.01) or mock infected. Uninfected viruses were washed out and human NK cells added at an effector/target ratio of 4:1. Twenty-four hours after NK cell addition, cells were imaged under fluorescent microscopy and harvested. Harvested cells were stained with the Live/Dead Fixable Dead Cell Stain Kit (Invitrogen) per the manufacturer's instruction and quantified using Becton Dickinson FACS LSR II (Becton Dickinson).

Animal surgery

All mouse experiments were housed and handled in accordance with the Subcommittee on Research Animal Care of the Ohio State University guidelines and have been approved by the Institutional Review Board. Female athymic nu/nu mice (Charles River Laboratories), 4-to 5-week-old for subcutaneous tumor model and 6-to 8-week-old for intracranial tumor model, were used for all studies.

For subcutaneous tumor studies, 1×10^6 CAL27 were implanted subcutaneously into the rear flank of nude mice. When tumors reached an average size of 100 mm^3, tumor-implanted mice were randomized and intraperitoneally treated with PBS or bortezomib (0.8 mg/kg) twice a week. Seven days after bortezomib treatment, PBS or 34.5ENVE were administered intratumorally (1×10^5 PFU).

For intracranial tumor studies, anesthetized nude mice were fixed in a stereotactic apparatus, and a burr hole was drilled at 2 mm lateral to the bregma, to a depth of 3 mm. A total 1×10^5 GBM30 cells were implanted in 4 μL Hank's buffered salt solution. Seventy-two hours following cell implantation, mice were randomized and treated with PBS or 0.8 mg/kg of bortezomib twice a week. Ten days after tumor cell implantation, mice anesthetized and stereotactically inoculated with 1×10^5 pfu of 34.5ENVE or PBS at the same location. For experiments involving autologous NK cell adjuvant therapy, NK cells isolated from human donors and 1×10^5 NK cells were stereotactically inoculated at the same location 13 days after tumor implant. Animals were observed daily and were euthanized at the indicated time points or when they showed signs of tumor burden (hunched posture and weight loss).

Histology and immunohistochemistry

Tumors were fixed in 4% buffered paraformaldehyde, followed by 30% sucrose at 4°C, embedded in OCT compound (Tissue Tek, Sakura Finetec) and cut into 10-μm sections. Representative sections were stained with hematoxylin and eosin (H&E) and then examined by light microscopy.

Statistical analysis

To compare two independent treatments for continuous endpoints such as viral titers, apoptosis, ROS, and necroptosis, a Student *t* test was used. A one-way ANOVA was used for multiple pairwise comparisons. To evaluate the synergistic interaction between bortezomib and oHSV, an interaction contrast or two-way ANOVA model was applied, using the Tukey method to correct for multiple comparisons. Synergistic effect represents that the combined treatment produced an effect (versus control) greater than the additive effect of two single treatments (vs. control, respectively). A log-rank test was used to compare survival curves for survival data and cox regression model was used to evaluate the interaction between bortezomib and oHSV on survival data. *P* values were adjusted for multiple comparisons by Holms' procedure. All data analyses were performed using GraphPad Prism statistical software. A *P* value of 0.05 or less was considered significant.

Results

Impact of bortezomib and oHSV on cell death

To understand the impact of bortezomib and oHSV treatment on the mechanism of cell death, we first evaluated their impact on cellular death and apoptosis by measring changes in cell killing upon treatment with bortezomib and/or oHSV. Although bortezomib treatment increased oHSV-infected GFP-positive cells and

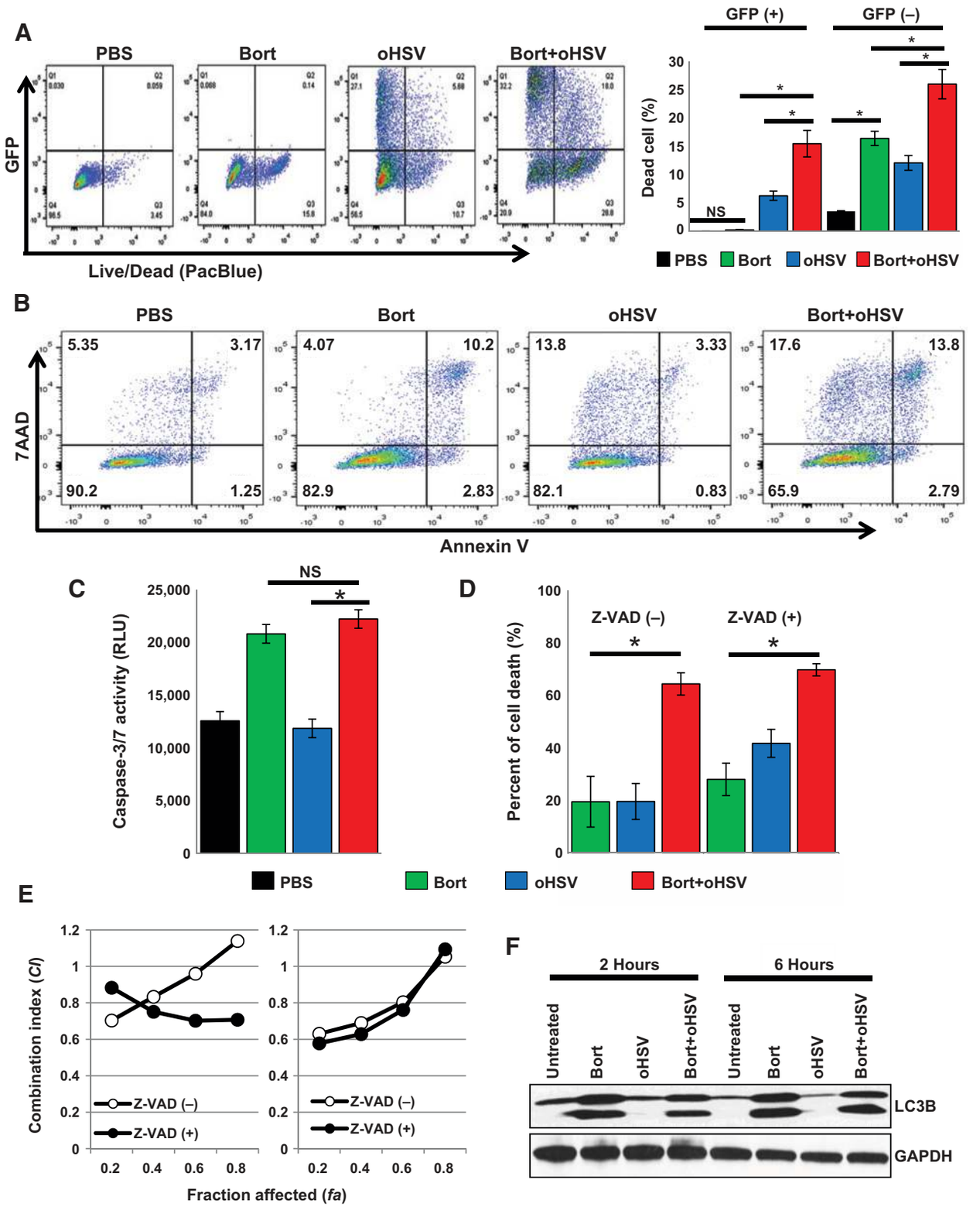

Figure 1.

Combination treatment-induced synergistic cell killing is independent of apoptotic and autophagic cell death. **A,** live/dead cell staining of infected (GFP^{+ve}), uninfected (GFP^{-ve}), bortezomib, and/or oHSV-treated cells. U251T3 glioma cells were pretreated with 12 nmol/L bortezomib for 16 hours before 34.5ENVE infection at an MOI of 0.01. After 24 hours, cells were harvested and stained with a live/dead fixable aqua dead cell staining solution. (*Continued on the following page.*)

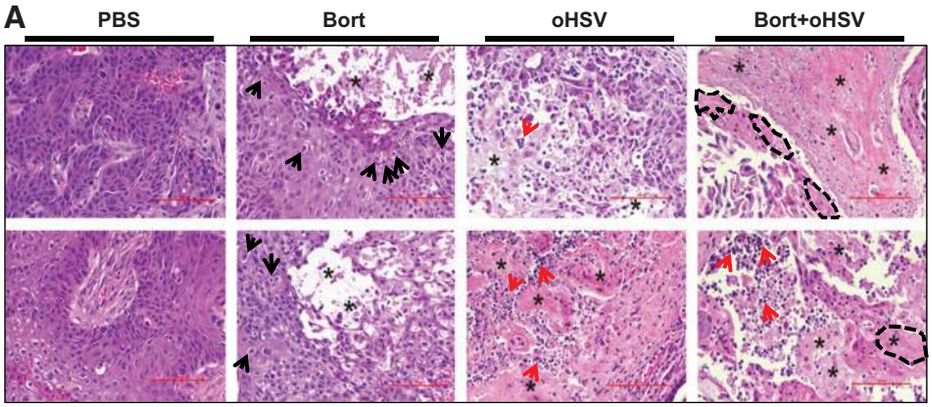

Figure 2.

Bortezomib and oHSV combination treatment induces necroptotic cell death *in vivo*. **A**, subcutaneously implanted CAL27 head and neck tumors from mice treated with bortezomib (0.8 mg/kg) and/or HBSS or 1×10^5 pfu of oHSV were harvested and sectioned 3 days after virus injection. Data shown are representative H&E-stained images of tumor sections from mice treated with PBS, bortezomib (Bort), oHSV, or the combination of Bortezomib and oHSV (Bort $^+$ oHSV). Black arrows indicate tumor cells with condensed nuclei, morphologic features associated with apoptosis. Red arrows indicate areas with extensive immune cell infiltration. Asterisks (*) indicate areas of necrotic tissue. Cells displaying characteristic features of karyohexis or karyolysis are encircled by a dotted line.

also synergistically increased total dead cells (Fig. 1A), a synergistic increase in the percentage of Annexin-positive apoptotic cells was not observed in combination-treated cells (Fig. 1B). Consistent with these results, no further increase in Caspase-3 activity was observed (Fig. 1C) in combination-treated cells versus bortezomib alone. Pretreatment of cells with Z-VAD-FMK, a pan Caspase inhibitor, did not affect the synergistic cell killing observed between bortezomib and oHSV (Fig. 1D and E). Taken together, these data suggest that treatment of oHSV-infected cells with bortezomib resulted in increased tumor cell killing by a mechanism that was independent of apoptosis.

Cellular autophagy is usually considered as a cellular stress response to counter cellular apoptosis (11) and dysregulated autophagy results in cell death with oncolytic adenoviruses (12). Because wild-type HSV infection can also initiate autophagy (13, 14), the cellular autophagic response was assessed by comparing the accumulation of LC3IIb in cells following treatment. Western blot analysis revealed no obvious change in LC3IIb accumulation in cells treated with the combination of oHSV and bortezomib, suggesting that changes in cellular autophagy likely did not contribute to the increased cell death observed in combination treated cells (Fig. 1F).

Analysis of hematoxylin and eosin (H&E)–stained sections of xenograft tumors from nude mice treated with bortezomib and/or oHSV revealed large geographic areas of necrosis in tumors from mice treated with both bortezomib and oHSV (Fig. 2). Tumors from mice treated with bortezomib showed condensed nuclei, a morphologic feature associated with apoptosis (black arrow heads). Although tumors from mice treated with oHSV alone showed evidence of necrosis, tumor tissues from mice treated with both bortezomib and/or oHSV displayed extensive areas of tumor necrosis throughout the tumor (asterisks) with extensive immune cell infiltration (red arrow heads). Tumor sections from combination treated mice revealed cells that appeared to have undergone karyohexis (fragmented DNA) or karyolysis (anuclear cells with absent chromatin) surrounding necrotic areas suggestive of necrotic tissue death (encircled with dotted lines). Collectively, these observations implied that combination treatment with bortezomib and oHSV possibly induced necroptic cell death, a mechanism of cell death that is distinct from the effects of either treatment alone on tumor cells.

Combination treatment with bortezomib and oHSV induces receptor interacting protein kinase 1 (RIPK1)–dependent necroptotic cell death

Necroptotic cell death is a mechanism of cell death that involves the formation of a receptor-interacting protein kinase 1 (RIPK1)–dependent complex that results in increased ROS and JNK activity that leads to a regulated necrosis-like cell death (Fig. 3A; ref. 11). Thus, we tested the involvement of necroptotic cell death in synergistic cell death of oHSV-infected cells after bortezomib treatment. Pretreatment with necrostatin-1 (Nec-1), an inhibitor of RIPK1, or molecular knockdown of RIPK1 significantly reduced the synergistic cell killing observed

(*Continued.*) Representative scatter plots and the mean percentage of dead cells in GFP^{+ve} and GFP^{-ve} population are indicated. **B,** Annexin V versus 7AAD scatter dot plots of bortezomib and/or oHSV treated cells. **C,** quantification of Caspase 3/7 activity measured using a caspase 3/7 activity assay kit. **D** and **E,** the effect of caspase inhibitor, Z-VAD-FMK, treatment was assessed on combination treatment-induced synergistic killing. U251T3 cells were pretreated with/without 20 μmol/L of Z-VAD-FMK for 1 hour, and then treated with serially diluted bortezomib. Sixteen hours later, drug was washed out and cells were treated with serially diluted 34.5ENVE. Bortezomib and 34.5ENVE were serially diluted at concentrations of 0.0625, 0.125, 0.25, 0.5, 1, 2, and 4 times their ED_{50} in a constant ratio. Seventy-two hours after34.5ENVE infection, cell viability was measured via MTT assay. **D,** data points represent the mean percentage cell viability relative to uninfected cells. **E,** effect of Z-VAD-FMK treatment on synergistic cell killing of tumor cells treated with bortezomib and oHSV. Data shown as fraction affected (fa) versus combination index (CI) plots. CI < 1 indicate synergy, CI = 1 indicate additive, and CI > 1 indicate antagonistic interaction. **F,** U251T3 cells were treated as in (**A**), and cells were harvested after 2 and 6 hours. Cell lysates were probed with antibodies against LC3B and GAPDH was used as a loading control. All flow cytometric analyses data are representative of three independent experiments. Errors bars represent ± SD for each group.

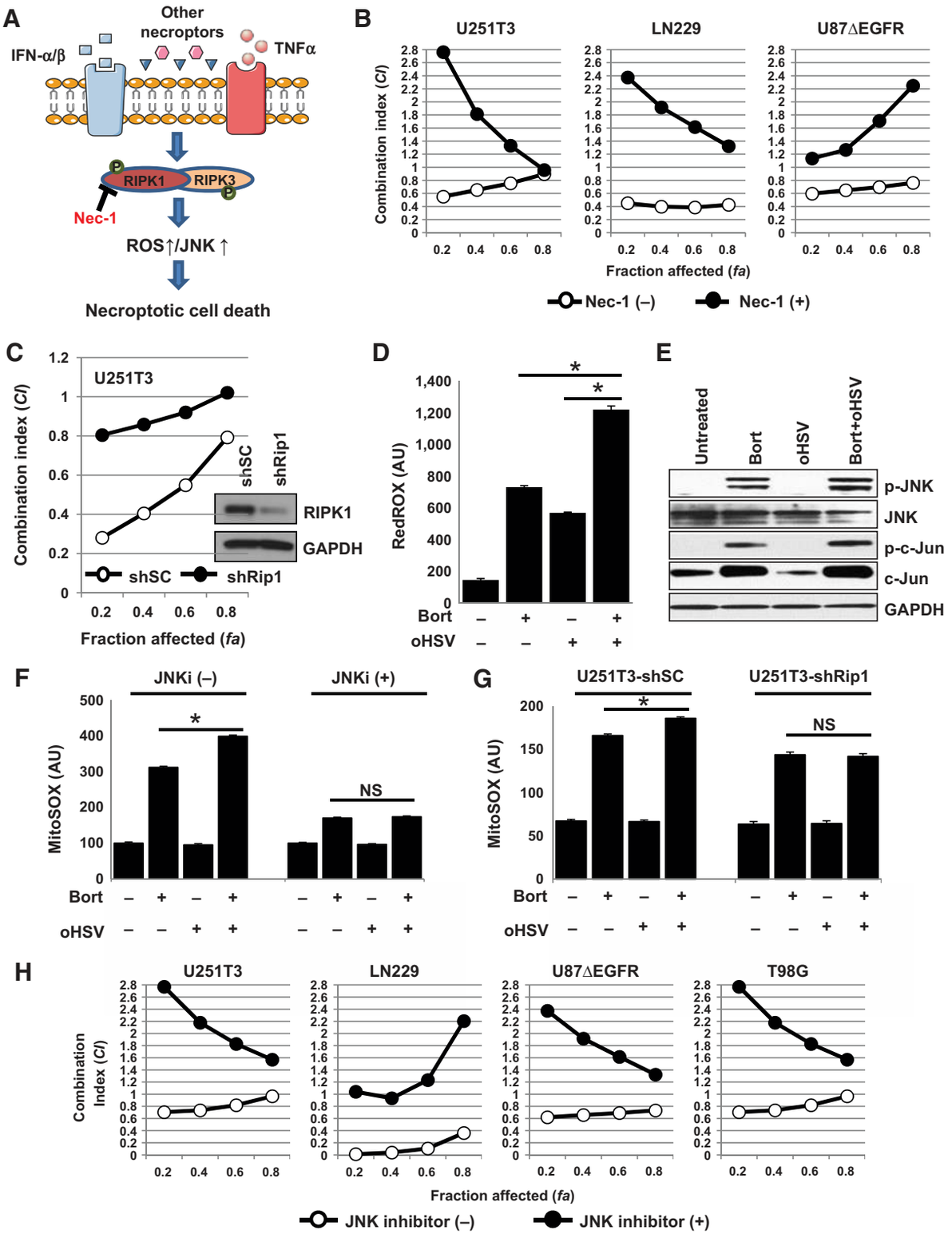

Figure 3.

Combination treatment with bortezomib and oHSV induces necroptotic cell death. **A,** schematic illustration of the necroptotic cell death pathway. **B** and **C,** the interaction between bortezomib and 34.5ENVE on cell killing was analyzed by the median-effect method of the Chou–Talalay analysis. Data are presented as fraction affected (fa) versus combination index (CI) plots with/without Necrostatin-1 (Nec-1; **B**) or with RIPK1 knockdown (**C**). (*Continued on the following page.*)

upon infection of bortezomib treated cells (Fig. 3B and C and Supplementary Fig. S1; ref. 15). Interestingly, both Nec-1 treatment and RIPK1 knockdown did not reduce the bortezomib-induced increase in virus replication (Supplementary Fig. S2), indicating a role for necroptosis in cell death but not virus replication following combinatorial treatment. Measurement of cellular ROS levels revealed significantly more ROS production in cells treated with bortezomib and oHSV compared with either agent alone (Fig. 3D).

The primary downstream effectors of RIPK1-induced necroptotic cell death are JNK activation and increased mitochondrial ROS (Fig. 3A; refs. 16, 17). Changes in JNK activation (Fig. 3E) and mitochondrial ROS production (Fig. 3F and G) were tested in U251T3 tumor cells treated with ED_{50} doses of bortezomib (12 nmol/L) followed by ED_{50} doses of oHSV (MOI = 0.01) infection. Western blot analysis revealed an increased phosphorylation of JNK and c-Jun upon treatment with both bortezomib and oHSV (Fig. 3E). Using a MitoSOX assay, a significant increase in mitochondrial-released ROS levels was observed in combination treated cells. However, pretreatment with either JNK inhibitor or RIPK1 knockdown reversed this increased mitochondrial ROS production in combination treated cells (Fig. 3F and G). Because JNK signaling contributes to necroptotic cell death, we assessed the role of JNK signaling on the combination treatment interaction. In all cell lines tested, JNK inhibition reduced the synergistic cell killing observed with combination treatment (Fig. 3H and Supplementary Fig. S1). Taken together, these data suggest that combination treatment with bortezomib and oHSV induced necroptotic cell death through the RIPK1–JNK pathway, and that this induction is essential to achieve synergistic cell killing after bortezomib and oHSV treatment.

Combination treatment activates proinflammatory pathways

Necroptotic cell death results in rapid plasma membrane permeabilization that activates and releases cytokines, such as IL1α, that can trigger vigorous inflammatory responses (18, 19). To investigate whether combination treatment-induced necroptotic cell death also increases proinflammatory cytokine secretion, we measured changes in secreted protein (Fig. 4A) of proinflammatory cytokine such as IL1α from tumor cells treated with bortezomib and oHSV *in vitro* and *in vivo* (Fig. 4). Increased IL1α secretion was observed *in vitro* and in the serum of GBM30 intracranial tumor-bearing mice treated with bortezomib and oHSV (Fig. 4B).

Combination-treated tumor cells activate NK cells

IL1α (observed after combination treatment above) has been previously shown to result in enhanced NK cell activity against tumor cells (20, 21). Thus, we investigated the impact of combination treatment of tumor cell sensitization to NK cell activity. Primary donor derived human NK cells from three different donors were cocultured with combination treated tumor cells for 24 hours. Enzyme linked immunosorbent assays (ELISA) were then used to assess IFNγ and TNFα secretion following coculture. Consistent with previous reports (22), NK cells cocultured with bortezomib-treated cells expressed and secreted significantly higher levels of TNFα and IFNγ versus controls (Fig. 5A and B). More importantly, combination treatment with bortezomib and oHSV resulted in a significant enhancement of both TNFα and IFNγ gene expression and cytokine secretion over either single-agent alone (Fig. 5A and B).

Tumor cell surface ligands can also initiate cross talk with NK cells to mediate their activity (23). Thus, we evaluated changes in both NK-activating ligands on tumor cells and NK cell activation markers on NK cells co-cultured with glioma cells treated with or without bortezomib in the presence or absence of oHSV. Flow cytometric analysis of NK cell–activating ligands on treated tumor cells revealed that bortezomib and combination treatment induced a significant increase in tumor cell surface expression of NK cell–activating receptors: CD58, CD112, and CD155 (Fig. 5C). Furthermore, an assessment of NK cell–activating receptors was conducted 24 hours post exposure to treated tumor cells. A significant increase in NK cell surface expression of CD69 and TRAIL was observed when cultured with combination-treated tumor cells versus each treatment alone (Fig. 5B and D).

NK cells are known to induce apoptosis of target cells. Thus, we investigated the effect of NK cells on tumor cell apoptosis. Immunoblot analysis for cleaved Caspase-8, cleaved Caspase-3, and cleaved PARP of glioma cells in the presence or absence of NK cells revealed increased activation of Caspase-8, Caspase-3, and PARP in combination treated tumor cells co-cultured with human donor NK cells, revealing enhanced tumor cell sensitivity to NK cell–mediated apoptotic death (Fig. 5E).

Bortezomib and oHSV treatment enhances NK cell anti-tumor effects *in vitro* and *in vivo*

Collectively, these results demonstrate that combination treatment induced necroptotic cell death accompanied by increased proinflammatory cytokine expression and NK cell activation. Thus, we tested whether we could harness the NK cell sensitivity of combination-treated tumors with NK cell adjuvant therapy. U251T3-mCherry cells were pretreated with or without bortezomib for 16 hours followed by oHSV treatment at an MOI of 0.01 (ED_{50}). Two hours later, cells were washed to remove unbound virus and then overlaid with

(*Continued.*) **D,** cellular ROS production was measured using a CellROX kit. U251T3 cells were treated with 12 nmol/L bortezomib for 16 hours before 34.5ENVE infection (MOI = 0.01). ROS was assessed 24 hours later. Data points represent the mean and error bars indicate ± SD confidence intervals for each group performed in triplicate. **E,** U251T3 glioma cells were pretreated with/without 12 nmol/L bortezomib for 16 hours and then infected with oHSV (MOI = 0.01). Cells were then harvested 2 and 6 hours later and probed with antibodies against phospho-JNK (p-JNK), total JNK, phospho-c-Jun (pc-Jun), and total c-Jun by western blot analysis. GAPDH was used as a loading control. **F,** specific mitochondrial ROS production was measured using the MitoSOX kit. U251T3 cells were pretreated with/without 10 μmol/L JNK inhibitor (SP0600125) and then treated with 12 nmol/L bortezomib for 16 hours before 34.5ENVE infection (MOI = 0.01). Mitochondrial ROS production was assessed 24 hours later. Data points represent the mean and error bars indicate ± SD confidence intervals for each group performed in triplicate. **G,** U251T3 cells were transduced with a RIPK1 shRNA- or non-targeting shRNA-expressing lentivirus. Stably transduced cells were then treated with 12 nmol/L bortezomib for 16 hours before 34.5ENVE infection (MOI = 0.01). Mitochondrial-specific ROS production was then assessed 24 hours later. Data are shown as mean and ± SD confidence interval of three replicates for each group. **H,** JNK inhibitor treatment rescued the synergistic cell death caused by combinatorial therapy. Cells were treated with SP0600125 (10 μmol/L) before bortezomib treatment (16 hours) and the interaction between bortezomib and oHSV on cell killing was analyzed by the median-effect method of the Chou–Talalay analysis. Data are presented as fraction affected (*fa*) versus combination index (CI) plots. A *P* value of 0.05 or less was considered significant. *, $P \leq 0.05$

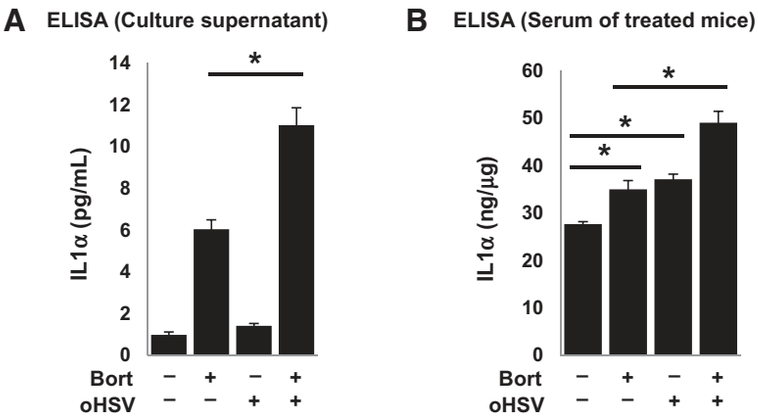

Figure 4.
Combination treatment-induced necroptotic cell death enhances proinflammatory cytokine secretion. **A**, ELISA quantification of secreted proinflammatory cytokine. U251T3 glioma cells were pretreated with 12 nmol/L bortezomib for 16 hours before 34.5ENVE infection at an MOI of 0.01. Six hours after 34.5ENVE infection, media were harvested and assessed for secreted IL-1α via ELISA. **B**, athymic nude mice were stereotactically implanted with patient derived primary GBM30 cells. Five days after tumor implantation mice were treated with PBS/bortezomib (0.8 mg/kg) via intraperitoneal route twice a week for the duration of the study. On day 10, 1×10^5 pfu of 34.5ENVE were intratumorally injected. Three days after 34.5ENVE treatment; murine serum was collected and assessed for secreted IL1α via ELISA. Data points represent the mean and error bars indicate ± SD for each group ($N = 5$/each group) performed in triplicate. A P value of 0.05 or less was considered significant. *, $P \leq 0.05$.

primary donor-derived human NK cells from two independent donors. Twenty-four hours later, cell killing was assessed via live/dead cell staining and FACS analysis. Glioma cell killing was significantly higher of glioma cells treated with bortezomib and oHSV after co-culture with NK cells from two different donors (a 1.9- and 2.1-fold increase compared to no NK cell co-culture samples) as indicated by FACS analysis (both mCherry and Pacblue positive; Fig. 6A and B). Consistent with previous reports, both bortezomib and oHSV as single-agent treatments also sensitized glioma cells to NK cell–mediated killing (Supplementary Fig. S3; ref. 24).

To test the therapeutic efficacy of this *in vivo*, intracranial tumor-bearing mice treated with bortezomib and oHSV were further treated with normal human NK cell adjuvant therapy and evaluated for survival. NK cell therapy significantly improved survival of mice treated with both bortezomib and oHSV (Fig. 6C). Taken together, these data indicate that (i) combination treatment-induced necroptotic cell death resulted in the activation of NK cells and (ii) NK cell adjuvant therapy enhanced therapeutic efficacy of mice.

Discussion

The recent approval of T-Vec for melanoma reflects the promising effects of biological therapy to treat some of the most aggressive cancers. We have previously demonstrated that the proteasome inhibitor bortezomib induced expression of HSP90 that supported nuclear localization of the viral polymerase, leading to increased virus replication and antitumor efficacy of oHSV. Therapeutic combination treatment strategies such as this result in a decrease in the doses of each treatment necessary, and thus hold promise for the treatment of solid tumors while minimizing toxicity (3). In our study, we found that combination treatment with bortezomib- and oHSV-sensitized tumor cells to exogenous cellular immunotherapy with primary NK cells. Because autologous NK cell immunotherapy for GBM patients (NCT00331526 and NCT01588769), Neukoplast or NK-92 therapy, and proteasome inhibitors are all being evaluated in patients (NCT00900809, NCT02465957, and NCT00990717). This study lays down the rationale for testing oHSV therapies in conjunction with NK cell therapy. Because oHSV is given by intratumoral injection, it would be feasible to infuse NK cells along with the virus by a direct injection into tumor site in patients given bortezomib systemically.

Although bortezomib induces ER stress and apoptosis, HSV-1 can hijack cellular pathways to override this response (25). Here, we found that oHSV infection of bortezomib-treated cells synergistically increased cell death independent of both apoptosis and/or autophagic cell death. Many standard cancer chemotherapeutic drugs, including bortezomib, doxorubicin, and cisplatin exert their anticancer activity by inducing cellular apoptosis. Resistance to apoptosis often occurs in patients and presents a challenge to the development of cancer therapeutics that rely on cellular suicide death mechanisms. Interestingly, because HSV-1–infected cells are resistant to apoptotic cell death, infected cells are primed to enter necroptotic cell death (26). In this study, we found that combination treatment of bortezomib and oHSV induces caspase-independent necroptotic cell death in glioma and highlights the therapeutic potential of this treatment for tumors that do not respond to traditional chemotherapies due to defects in proapoptotic signaling. It is important to note that bortezomib is thought to have very low BBB penetration (27). Consistent with this finding, we did not observe any improvement in the survival of mice bearing intracranial tumors treated with this single agent (Supplementary Fig. S4). However, we have previously demonstrated increased vascular leakiness in tumors after oHSV therapy (28). It is thus interesting to speculate if oHSV therapy can also be exploited to improve penetration of drugs, such as bortezomib, into tumors where with limited penetration.

Apoptotic cell death is accompanied by membrane blebbing, resulting in apoptotic bodies that are engulfed by phagocytes and thus culminating in an immunologically silent death (29, 30). Necrotic cells, however, undergo a rapid loss of membrane integrity that allows the release of cytokines, resulting in a robust inflammatory response (31–34), which can ultimately result in an antitumoral immune response. Our results indicate that necroptotic cell death is a cell death mechanism downstream of virus replication and its blockade does not affect oHSV replication *in vitro* (Supplementary Fig. S2). Interestingly, necroptotic cell death–associated inflammation can also serve as a mechanism for pathogen clearance (18). Here, we observed a significant induction of the secretion of several cytokines, such as IL1α in combination treated tumors *in vitro* and *in vivo*. These findings suggest that this enhanced inflammatory response may herald a significant and long-term antitumor immune response. Bortezomib treatment has also been proven to sensitize human and mouse tumor cells to TRAIL and/or NK cell–mediated killing through the expression of apoptosis-inducing death receptors,

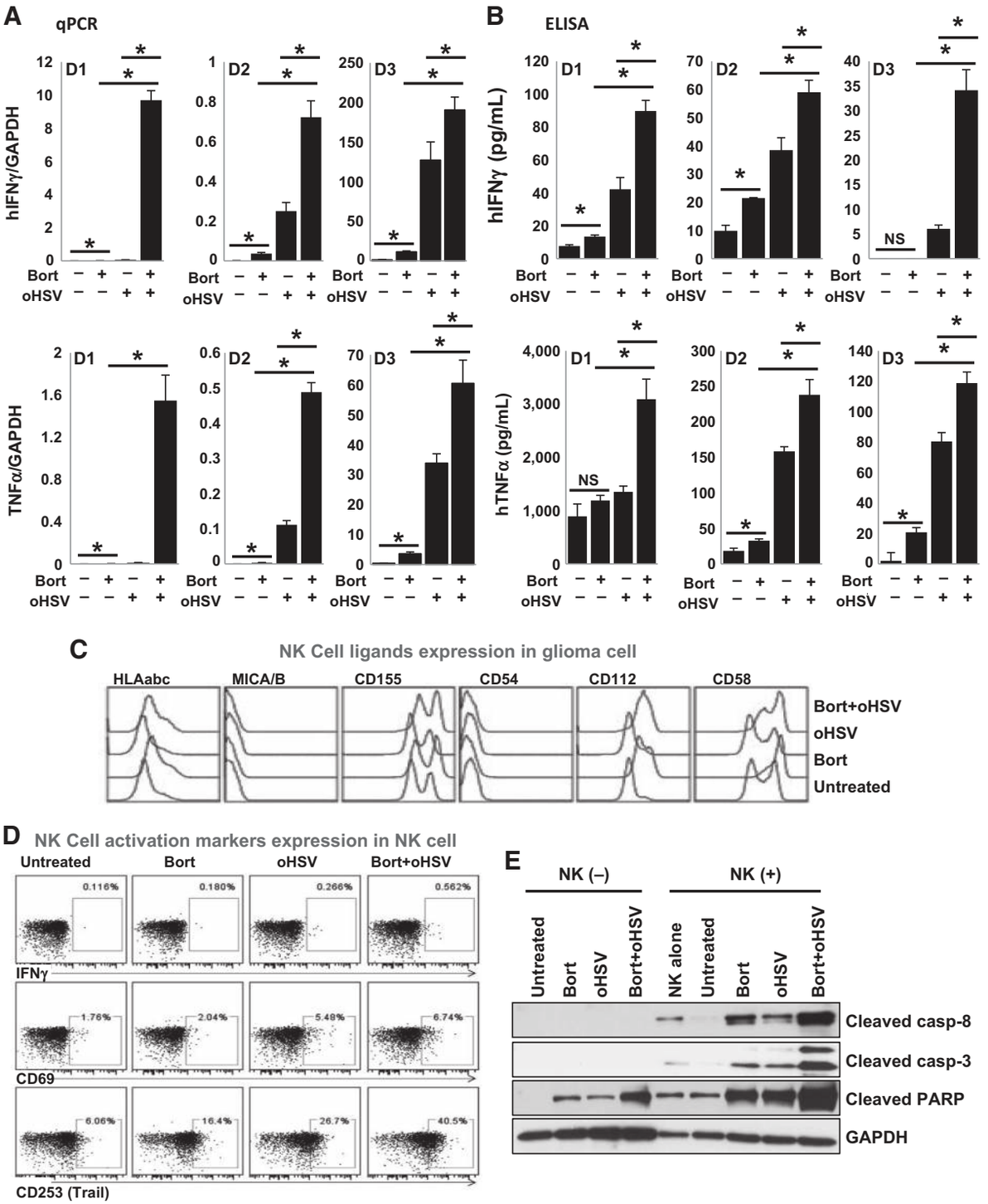

Figure 5.

Bortezomib and oHSV therapy enhances NK cell activation. **A** and **B,** U251T3-mCherry^{+} glioma cells were pretreated with 12 nmol/L bortezomib 16 hours before 34.5ENVE infection at an MOI of 0.01. Two hours after 34.5ENVE infection, unbound virus was washed out and cells were overlaid with/without primary human NK cells from three independent donors (D1, D2, and D3). Twenty-four hours later, culture supernatants were analyzed for TNFα and IFNγ gene expression and secretion by Q-PCR (**A**) and ELISA (**B**). **C,** flow cytometric analysis of NK cell activating ligands (HLA abc, MICA/B, CD155, CD54, CD112, and CD58) on tumor cells after treatment with bortezomib and/or oHSV as indicated. **D,** flow cytometric analysis of NK cell–activating receptors TRAIL and CD69 as well as intracellular IFNγ after co-culture with treated tumor cells as indicated. **E,** Western blot analysis of the cleavage of caspases 8, 3, and PARP in treated tumor cells co-cultured with primary NK cells. GAPDH was used as a loading control. A P value of 0.05 or less was considered significant. *, $P \leq 0.05$.

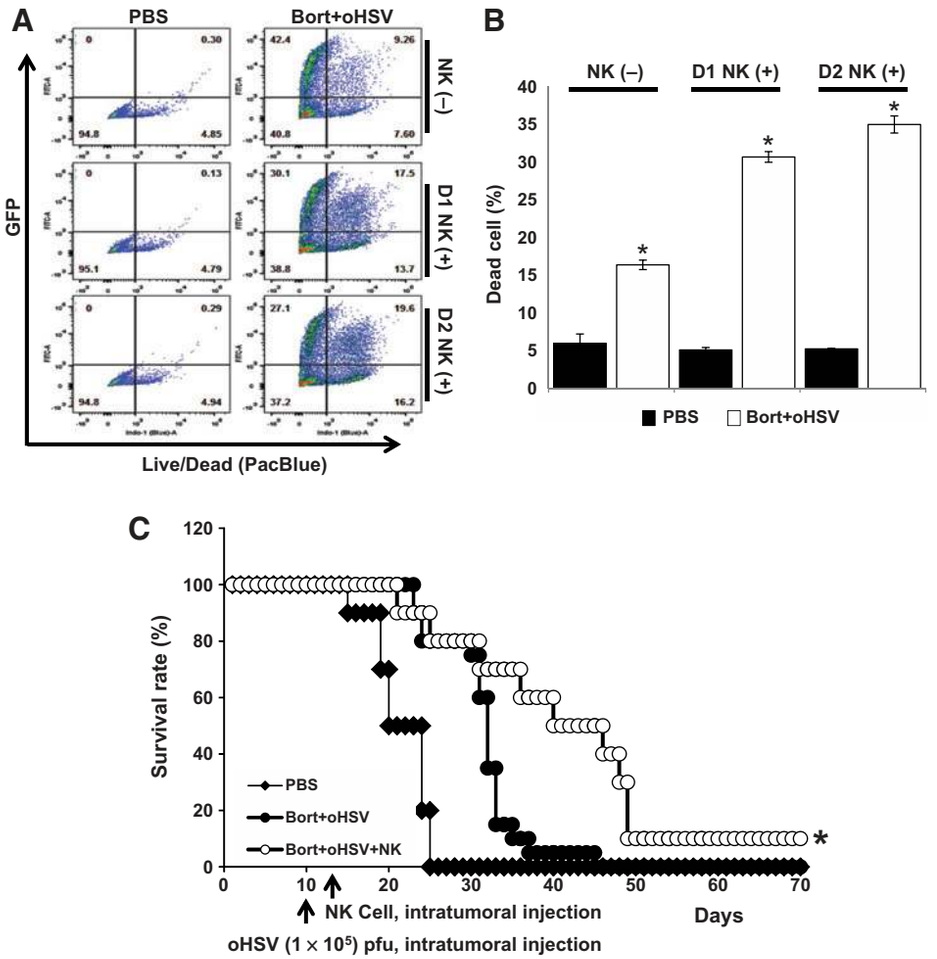

Figure 6.
Combination therapy significantly enhances NK cell adjuvant therapy. **A** and **B,** U251T3-mCherry$^+$ cells were pretreated with or without bortezomib for 16 hours followed by oHSV treatment at an MOI of 0.01. Two hours after oHSV infection, unbound virus was washed out and cells were then overlaid with primary human NK cells from two independent donors. Twenty-four hours later, cells were harvested and stained with a live/dead fixable aqua dead cell staining solution. **A,** representative quadrant plots of live/dead cells and viral GFP after gating on mCherry-positive cells. **B,** the mean percentage positive number of dead cells following co-culture with primary NK cells (after mCherry$^+$ gating). Errors bars represent ± SD for each group. **C,** athymic nude mice bearing intracranial GBM30 tumors were treated with bortezomib (0.8 mg/kg) intraperitoneally twice a week for the duration of the study and oHSV on day 10 aftert tumor implantation. NK cell adjuvant therapy was conducted using fresh primary human NK cells via intratumoral injection of 1×10^5 primary NK cells 3 days after oHSV treatment. Mice were then monitored for survival. Kaplan–Meier survival curves of animals in each group ($N = 10$ for PBS, Bort+oHSV, and Bort+oHSV+NK cell) are indicated. A P value of 0.05 or less was considered significant. *, $P \leq 0.05$.

such as DR5 (22, 24). NK cells are innate lymphocytes capable of mediating cytotoxicity against tumor and virally infected cells and do not require the presence of a specific tumor antigen for recognition (35). Alternatively, others have also reported that bortezomib can have NK cell immunosuppressive effects by inhibiting cellular proliferation (36, 37). In this study, we report increased expression of NK cell–activating receptors CD155, CD112, and CD58 after exposure to proteasome inhibitor. More significantly, the increased expression of these NK-activating cell surface markers was retained after oHSV infection of bortezomib treated cells. Coculture of NK cells with combination treated tumor cells also resulted in increased NK cell TNFα and IFNγ secretion, as well as NK cell–mediated apoptosis.

The impact of NK cells on combination therapy was also assessed *in vivo*. NK cell adjuvant therapy resulted in significant enhancement of murine survival following bortezomib and oncolytic virus treatment in tumor-bearing mice. We and others have previously shown that modulation of host immune responses can limit intratumoral infiltration of innate immune response mediators, such macrophages and NK cells, and thereby result in increased viral propagation and enhanced antitumor efficacy (10, 38, 39). We have also recently shown that elevated TNFα production in the tumor microenvironment leads to oHSV-infected cell apoptosis and can limit viral replication and efficacy (40). We hypothesize that a major limitation to exploiting endogenous NK cells to augment immunotherapy of infected tumors is likely due to low effector to target cell ratios. Here, we show NK cell adjuvant therapy can be exploited to enhance the NK:infected tumor cell ratio and result in increased tumor cell sensitivity to NK cell–mediated killing that can augment combination therapy. In bortezomib- and oHSV-treated mice, NK cell adjuvant therapy resulted in a significant enhancement of the survival of glioma bearing mice. It would be important to note that as virus treatments in combination with agents that enhance oncolysis and/or immunotherapeutic effects are translated into patients, we might uncover previously unidentified toxicities that might be due to virus dose amplifications or increases in an inflammatory response. Although both viral dose amplifications as well as severe inflammatory responses can be checked by antiherpetic treatments and steroids or other anti-inflammatories there would be a need to monitor these patients carefully for potential signs of toxicity. Recent studies have highlighted the contextually dependent effects of the host innate antiviral response: which can be detrimental when mediating virus clearance, but beneficial in activating antitumor responses (41). To our knowledge, this is the first study to exploit NK cell adjuvant therapy in combination with virotherapy and proteasome blockade. Because proteasome inhibitors, oHSV, and autologous NK cell immunotherapy are currently being investigated

individually in GBM patients, our study may help guide the future clinical development of novel combination therapies for GBM.

Disclosure of Potential Conflicts of Interest

No potential conflicts of interest were disclosed.

Authors' Contributions

Conception and design: J.Y. Yoo, A.C. Jaime-Ramirez, B.S. Hurwitz, M.T. Lotze, J. Yu, M.A. Caligiuri, M. Old, B. Kaur
Development of methodology: J.Y. Yoo, A.C. Jaime-Ramirez, C. Bolyard, T. Nallanagulagari, T. Relation, C.M. Croce, M. Old, B. Kaur
Acquisition of data (provided animals, acquired and managed patients, provided facilities, etc.): J.Y. Yoo, A.C. Jaime-Ramirez, C. Bolyard, H. Dai, T. Nallanagulagari, J. Wojton, T. Relation, J.-G. Yu, C.M. Croce
Analysis and interpretation of data (e.g., statistical analysis, biostatistics, computational analysis): J.Y. Yoo, A.C. Jaime-Ramirez, C. Bolyard, J. Wojton, T. Relation, J. Zhang, J. Yu, M.A. Caligiuri, M. Old, B. Kaur
Writing, review, and/or revision of the manuscript: J.Y. Yoo, A.C. Jaime-Ramirez, C. Bolyard, J. Wojton, T. Relation, M.T. Lotze, J. Yu, B. Kaur
Administrative, technical, or material support (i.e., reporting or organizing data, constructing databases): C. Bolyard, T.J. Lee, M.T. Lotze
Study supervision: J.Y. Yoo, C.M. Croce, M.A. Caligiuri, M. Old, B. Kaur

Grant Support

This work was supported by: R01 NS064607, P30 CA016058, R01 CA150153, P30 NS045758 (to B. Kaur); IRG-67-003-50 (to J.Y. Yoo); CA 186542-01A1 (to A.C. Jaime-Ramirez), T32 CA009338 (to C. Bolyard), P01CA163205 (to B. Kaur and M. Caligiuri) and Pelotonia Fellowship Program (to A.C. Jaime-Ramirez, H. Dai, and T. Nallanagulagari).

The costs of publication of this article were defrayed in part by the payment of page charges. This article must therefore be hereby marked *advertisement* in accordance with 18 U.S.C. Section 1734 solely to indicate this fact.

Received April 20, 2016; revised June 4, 2016; accepted June 21, 2016; published OnlineFirst July 7, 2016.

References

1. Kanai R, Wakimoto H, Cheema T, Rabkin SD. Oncolytic herpes simplex virus vectors and chemotherapy: are combinatorial strategies more effective for cancer? Future Oncol 2010;6:619–34.
2. Cvek B, Dvorak Z. The ubiquitin-proteasome system (UPS) and the mechanism of action of bortezomib. Curr Pharm Des 2011;17:1483–99.
3. Yoo JY, Hurwitz BS, Bolyard C, Yu JG, Zhang JY, Selvendiran K, et al. Bortezomib-induced unfolded protein response increases oncolytic HSV-1 replication resulting in synergistic antitumor effects. Clin Cancer Res 2014;20:3787–98.
4. Hui B, Shi YH, Ding ZB, Zhou J, Gu CY, Peng YF, et al. Proteasome inhibitor interacts synergistically with autophagy inhibitor to suppress proliferation and induce apoptosis in hepatocellular carcinoma. Cancer 2012;118: 5560–71.
5. Narita Y, Nagane M, Mishima K, Huang HJ, Furnari FB, Cavenee WK. Mutant epidermal growth factor receptor signaling down-regulates p27 through activation of the phosphatidylinositol 3-kinase/Akt pathway in glioblastomas. Cancer Res 2002;62:6764–9.
6. Yoo JY, Haseley A, Bratasz A, Chiocca EA, Zhang JY, Powell K, et al. Antitumor efficacy of 34.5ENVE: a transcriptionally retargeted and "Vstat120"-expressing oncolytic virus. Mol Ther 2012;20:287–97.
7. Bolyard C, Yoo JY, Wang PY, Saini U, Rath KS, Cripe TP, et al. Doxorubicin synergizes with 34.5ENVE to enhance antitumor efficacy against metastatic ovarian cancer. Clin Cancer Res 2014;20:6479–94.
8. Yoo JY, Pradarelli J, Haseley A, Wojton J, Kaka A, Bratasz A, et al. Copper chelation enhances antitumor efficacy and systemic delivery of oncolytic HSV. Clin Cancer Res 2012;18:4931–41.
9. Racoma IO, Meisen WH, Wang QE, Kaur B, Wani AA. Thymoquinone inhibits autophagy and induces cathepsin-mediated, caspase-independent cell death in glioblastoma cells. PLoS ONE 2013;8: e72882.
10. Alvarez-Breckenridge CA, Yu JH, Price R, Wojton J, Pradarelli J, Mao HY, et al. NK cells impede glioblastoma virotherapy through NKp30 and NKp46 natural cytotoxicity receptors. Nat Med 2012;18:1827–34.
11. Wojton J, Meisen WH, Kaur B. How to train glioma cells to die: molecular challenges in cell death. J Neurooncol 2016;126:377–84.
12. Klein SR, Piya S, Lu Z, Xia Y, Alonso MM, White EJ, et al. C-Jun N-terminal kinases are required for oncolytic adenovirus-mediated autophagy. Oncogene 2015;34:5295–301.
13. Lussignol M, Queval C, Bernet-Camard MF, Cotte-Laffitte J, Beau I, Codogno P, et al. The herpes simplex virus 1 Us11 protein inhibits autophagy through its interaction with the protein kinase PKR. J Virol 2013;87:859–71.
14. Orvedahl A, Alexander D, Talloczy Z, Sun QH, Wei YJ, Zhang W, et al. HSV-1ICP34.5 confers neurovirulence by targeting the Beclin 1 autophagy protein. Cell Host Microbe 2007;1:23–35.
15. Christofferson DE, Yuan JY. Necroptosis as an alternative form of programmed cell death. Curr Opin Cell Biol 2010;22:263–8.
16. Papa S, Bubici C, Zazzeroni F, Pham CG, Kuntzen C, Knabb JR, et al. The NF-kappa B-mediated control of the JNK cascade in the antagonism of programmed cell death in health and disease. Cell Death Differ 2006; 13:712–29.
17. Vande Walle L, Wirawan E, Lamkanfi M, Festjens N, Verspurten J, Saelens X, et al. The mitochondrial serine protease HtrA2/Omi cleaves RIP1 during apoptosis of Ba/F3 cells induced by growth factor withdrawal. Cell Res 2010;20:421–33.
18. Kaczmarek A, Vandenabeele P, Krysko DV. Necroptosis: the release of damage-associated molecular patterns and its physiological relevance. Immunity 2013;38:209–23.
19. Meng L, Jin W, Wang X. RIP3-mediated necrotic cell death accelerates systematic inflammation and mortality. Proc Natl Acad Sci U S A 2015; 112:11007–12.
20. Marhaba R, Nazarenko I, Knofler D, Reich E, Voronov E, Vitacolonna M, et al. Opposing effects of fibrosarcoma cell-derived IL-1 alpha and IL-1 beta on immune response induction. Int J Cancer 2008;123:134–45.
21. Mishra R, Polic B, Welsh RM, Szomolanyi-Tsuda E. Inflammatory cytokine-mediated evasion of virus-induced tumors from NK cell control. J Immunol 2013;191:961–70.
22. Lundqvist A, Abrams SI, Schrump DS, Alvarez G, Suffredini D, Berg M, et al. Bortezomib and depsipeptide sensitize tumors to tumor necrosis factor-related apoptosis-inducing ligand: a novel method to potentiate natural killer cell tumor cytotoxicity. Cancer Res 2006;66:7317–25.
23. Lundqvist A, Yokoyama H, Smith A, Berg M, Childs R. Bortezomib treatment and regulatory T-cell depletion enhance the antitumor effects of adoptively infused NK cells. Blood 2009;113:6120–7.
24. Hallett WH, Ames E, Motarjemi M, Barao I, Shanker A, Tamang DL, et al. Sensitization of tumor cells to NK cell-mediated killing by proteasome inhibition. J Immunol 2008;180:163–70.
25. Mulvey M, Arias C, Mohr I. Maintenance of endoplasmic reticulum (ER) homeostasis in herpes simplex virus type 1-infected cells through the association of a viral glycoprotein with PERK, a cellular ER stress sensor. J Virol 2007;81:3377–90.
26. Jerome KR, Fox R, Chen Z, Sears AE, Lee HY, Corey L. Herpes simplex virus inhibits apoptosis through the action of two genes, Us5 and Us3. J Virol 1999;73:8950–7.
27. Di K, Lloyd GK, Abraham V, MacLaren A, Burrows FJ, Desjardins A, et al. Marizomib activity as a single agent in malignant gliomas: ability to cross the blood–brain barrier. Neuro Oncol 2016;18:840–8.
28. Kurozumi K, Hardcastle J, Thakur R, Yang M, Christoforidis G, Fulci G, et al. Effect of tumor microenvironment modulation on the efficacy of oncolytic virus therapy. J Natl Cancer Inst 2007;99:1768–81.
29. Nagata S, Hanayama R, Kawane K. Autoimmunity and the clearance of dead cells. Cell 2010;140:619–30.
30. Lauber K, Blumenthal SG, Waibel M, Wesselborg S. Clearance of apoptotic cells: getting rid of the corpses. Mol Cell 2004;14:277–87.

31. Fadok VA, Bratton DL, Rose DM, Pearson A, Ezekewitz RA, Henson PM. A receptor for phosphatidylserine-specific clearance of apoptotic cells. Nature 2000;405:85–90.
32. Golstein P, Kroemer G. Cell death by necrosis: towards a molecular definition. Trends Biochem Sci 2007;32:37–43.
33. Zong WX, Thompson CB. Necrotic death as a cell fate. Genes Dev 2006; 20:1–15.
34. Pasparakis M, Vandenabeele P. Necroptosis and its role in inflammation. Nature 2015;517:311–20.
35. Herberman RB, Ortaldo JR. Natural killer cells: their roles in defenses against disease. Science 1981;214:24–30.
36. Chang CL, Hsu YT, Wu CC, Yang YC, Wang C, Wu TC, et al. Immune mechanism of the antitumor effects generated by bortezomib. J Immunol 2012;189:3209–20.
37. Berges C, Haberstock H, Fuchs D, Miltz M, Sadeghi M, Opelz G, et al. Proteasome inhibition suppresses essential immune functions of human $CD4^+$ T cells. Immunology 2008;124:234–46.
38. Haseley A, Boone S, Wojton J, Yu L, Yoo JY, Yu J, et al. Extracellular matrix protein CCN1 limits oncolytic efficacy in glioma. Cancer Res 2012;72: 1353–62.
39. Thorne AH, Meisen WH, Russell L, Yoo JY, Bolyard CM, Lathia JD, et al. Role of cysteine-rich 61 protein (CCN1) in macrophage-mediated oncolytic herpes simplex virus clearance. Mol Ther 2014;22:1678–87.
40. Meisen WH, Wohleb ES, Jaime-Ramirez AC, Bolyard C, Yoo JY, Russell L, et al. The impact of macrophage- and microglia-secreted TNFalpha on oncolytic HSV-1 therapy in the glioblastoma tumor microenvironment. Clin Cancer Res 2015;21:3274–85.
41. Meisen WH, Kaur B. How can we trick the immune system into overcoming the detrimental effects of oncolytic viral therapy to treat glioblastoma? Expert Rev Neurother 2013;13:341–3.